

The influence of orographic Rossby and gravity waves on rainfall

Naftali Y. Cohen* and William R. Boos 

Department of Geology and Geophysics, Yale University, New Haven, CT, USA

*Correspondence to: N. Y. Cohen, Lamont-Doherty Earth Observatory, 61 Route 9W, Palisades, NY 10964, USA.
E-mail: ncohen@ldeo.columbia.edu

Orography is known to influence winter precipitation in Asia and the Indo-Pacific Ocean by mechanically forcing winds, but the dynamics involved in the precipitation response are incompletely understood. This study investigates how two types of orographically forced oscillatory motions alter time-mean winds and precipitation. The quasi-geostrophic omega equation is used together with previous ideas of ‘downward control’ to develop a simple theory of the spatial distribution and amplitude of the vertical motion response to orographically forced stationary Rossby waves and gravity wave drag in a precipitating atmosphere. This theory is then used to understand the response of the boreal winter atmosphere to realistic Asian orography in a global numerical model that includes representations of moist processes and unresolved gravity wave drag. We isolate the effects of the orographically forced stationary Rossby wave and the gravity wave drag by incremental addition of wave sources in this model. The peak precipitation response to the forced Rossby wave is about a factor of three larger than that of the gravity wave drag, but the wave drag response has a distinct spatial structure that dominates in some regions. Both the Rossby wave and the gravity wave drag perturb precipitation in areas distant from orography, producing shifts in the equatorial intertropical convergence zone, an increase in precipitation over southern Asia, and drying in much of northern Asia.

Key Words: Rossby waves; gravity waves; orography; rainfall; omega equation; Tibetan Plateau; moisture

Received 28 June 2016; Revised 24 October 2016; Accepted 21 November 2016; Published online in Wiley Online Library 5 February 2017

1. Introduction

The mountains and plateaux of Asia, which form the largest expanse of elevated terrain on Earth, are known to exert a significant influence on precipitation during boreal summer and on the jet stream during winter. During summer, elevated terrain heats the troposphere and inhibits the horizontal mixing of dry and moist air, creating local and planetary-scale perturbations of rainfall (reviews by Yanai and Wu, 2006; Boos, 2015). In winter, a broad spectrum of oscillatory motions are excited when the jet stream impinges on Asian orography; standing Rossby waves stretch around Earth’s circumference (Held *et al.*, 2002) and smaller-scale gravity waves propagate vertically to break in the upper atmosphere, decelerating the mean zonal flow there (e.g. Teixeira, 2014; Cohen *et al.*, 2014). Despite much previous study of orographically forced Rossby and gravity waves, little attention has been given to the precipitation perturbations that accompany these oscillatory motions.

It may at first seem logical that most work on orographically excited waves has focused primarily on horizontal flow (e.g. Nigam *et al.*, 1988; Cook and Held, 1992) or on vertical velocities local to mountain slopes (e.g. Trenberth and Chen, 1988; Rodwell and Hoskins, 2001), because humidities are low and precipitation is thus small over most continental interiors during boreal winter (e.g. Figure 1(a)), when the mean flow that impinges on orography

is strong. However, precipitation rates are high over the ocean surrounding Asia, and there is a high degree of zonal asymmetry in precipitation in the Asian region during winter. Parts of continental Asia (e.g. eastern China) and much of the Indian and West Pacific Oceans receive more than half their annual rainfall during winter (Figure 1(b)). Does orography exert a non-local influence on the spatial distribution of winter precipitation over and around Asia?

Orographically forced Rossby waves can be understood using potential vorticity conservation: when air flows over elevated terrain, the height of the air column changes so that planetary and relative vorticity must change to conserve potential vorticity. For westerly flows, this results in a succession of large-scale vortices to the east of the terrain (e.g. Holton and Hakim, 2014, chapter 4). After some time, this wave train circumnavigates the planet and achieves a fixed pattern. In the presence of a temperature gradient, such as that which exists between Earth’s Equator and its poles, these vortices will be accompanied by vertical motions according to the diagnostic ω equation (e.g. Holton and Hakim, 2014, chapter 6). In a moist environment, one also needs to account for condensation and precipitation; if precipitation can be thought to reduce the effective static stability in ascending regions, moisture might then amplify vertical motions in the wave.

Elements of this picture of moist, quasi-geostrophic ascent in orographically forced stationary Rossby waves have been invoked in previous studies, though often without clear reference to

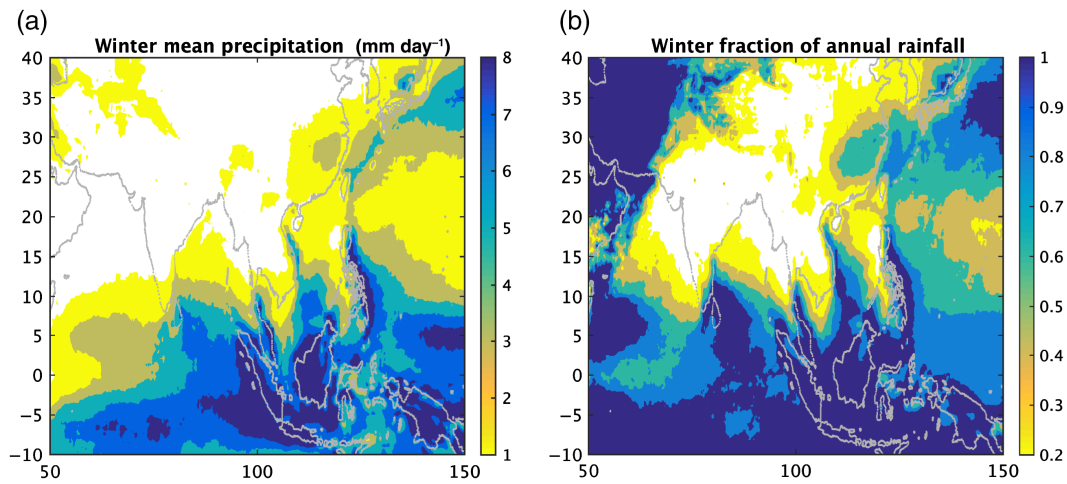


Figure 1. (a) The November–March mean precipitation (mm day^{-1}) and (b) its fractional contribution to the local annual mean rainfall using TRMM 3B42 (v7) daily data averaged over 1998–2012 with a horizontal resolution of $0.25^\circ \times 0.25^\circ$. Shading starts at (a) 1 mm day^{-1} and (b) 0.2, with white regions having smaller values. [Colour figure can be viewed at wileyonlinelibrary.com].

the wave dynamics. Manabe and Terpstra (1974) showed that orography increased the zonal variability of precipitation in a 45 day time-average of one general circulation model (GCM). In particular, orography decreased precipitation over southern Asia but increased precipitation over the West Pacific during their boreal winter simulation (their Figure 9.1). Broccoli and Manabe (1992) found that during boreal winter in a GCM, large-scale subsidence and infrequent storm development occurred upstream of the troughs of orographically induced stationary waves, contributing to dryness in the continental interiors of North America and Asia. Wills and Schneider (2016) showed that an idealized midlatitude mountain in a GCM with otherwise zonally symmetric boundary conditions produced a Rossby wave train that perturbed time-mean atmospheric moisture convergence (i.e. precipitation minus evaporation, $P - E$) from the midlatitudes all the way to the Equator. They explained how most of this hydrological response could be explained as the precipitation needed to balance the vertical flux of moisture by a time-mean ascent in the stationary wave. None of these studies drew a direct connection between vortices in stationary Rossby waves and the quasi-geostrophic ascent expected to occur downshear of cyclonic parts of these waves; making such a connection is one of the goals of this article.

Another goal is to examine the precipitation response to orographically forced Rossby and gravity waves in a unified framework. Orographic gravity waves (GWs) propagate vertically across stratification surfaces and transfer angular momentum from their source to higher levels where they break, typically decelerating the flow (e.g. Bühler, 2014). Because of their typically small horizontal scales (about 1–10 km), GCMs cannot resolve their influence and must parametrize their effects on the resolved flow (e.g. Alexander *et al.*, 2010). Most studies of orographic gravity wave drag (OGWD) have focused on the zonal mean (e.g. Palmer *et al.*, 1986; McFarlane, 1987; Stephenson, 1994). Yet Broccoli and Manabe (1992) showed that parametrized OGWD in their GCM enhanced the dryness of central Eurasia and contributed to other changes in annual mean precipitation. Recently, Shaw and Boos (2012) and Boos and Shaw (2013) used idealized analytical and numerical solutions to understand better how an upper-tropospheric westward torque, such as that produced by OGWD, can produce local perturbations to precipitation. Shaw and Boos (2012) showed that the vertical motion response to an upper-level, subtropical westward torque confined to a band of longitudes consists of ascent on the equatorward side of the torque and subsidence on the poleward side. Boos and Shaw (2013) showed that these vertical motions were amplified in a precipitating atmosphere and that subtropical, upper-level torques could induce non-local perturbations in near-equatorial precipitation.

Although we are interested in the precipitation induced by orographic waves in general, we focus on the effects of Asian orography because it provides the largest source of OGWD and stationary Rossby waves on Earth (Held *et al.*, 2002; Cohen and Boos, 2016). We examine boreal winter conditions because the flow over Asian orography is stronger during that season and thus excites greater wave activity. We will show that orographic Rossby waves influence precipitation over both Asia and the surrounding ocean and that OGWD also contributes significantly and distinctly to the organization of precipitation. To be clear, the effects of Asian orography on precipitation and winds during boreal summer involve an entirely separate set of mechanisms outside the scope of this article; mountains and plateaus act as a heat source to drive local precipitation (Wu *et al.*, 2012), and they also strengthen the interhemispheric south Asian monsoon by insulating its thermal maximum from the drying effects of extratropical air (e.g. Ma *et al.*, 2014; Boos, 2015).

This article is structured as follows: the next section details the comprehensive atmospheric model used in this study. In section 3 we summarize the implications of the quasi-geostrophic ω equation for the stationary Rossby wave response to an idealized orographic forcing, with an emphasis on the effects of moisture. A theoretical framework is also constructed to estimate the moist response to orographically induced gravity waves. Section 4 compares these estimates with results from the comprehensive atmospheric model that includes parametrized gravity waves and that accounts for moist processes. We focus on precipitation changes caused by the forced waves. We conclude and summarize our findings in section 5.

2. Methods

We use the atmospheric and land components of the Community Earth System Model (CESM) version 1.0.4. CESM is a comprehensive global climate model sponsored by the National Science Foundation and the US Department of Energy. We integrate the model with prescribed sea surface temperature, land ice, and sea ice, all with cyclic climatology but with no interannual variability. The horizontal resolution is about $1^\circ \times 1^\circ$ in the horizontal, with 42 vertical levels extending into the upper stratosphere. Here we present analyses of the last 40 years of 41-year long integrations. The OGWD parametrization used in the model is based on McFarlane (1987).

We use three integrations to investigate the effect of waves forced by flow over Asian orography. In the first, we remove (flatten) the Tibetan Plateau and other orography within the region $60\text{--}135^\circ\text{E}$, $22\text{--}55^\circ\text{N}$, and eliminate any tendencies produced by the OGWD parametrization in the same region. We refer to this integration as ‘FLAT’. In the second integration,

we maintain all orography but keep the OGWD parametrization turned off in the aforementioned region (we call this integration ‘TOPO’). In the third integration, which is effectively a control, we maintain both the large-scale topography and the OGWD parametrization (denoted by ‘TOPO+GW’). We isolate the effects of large-scale orographic Rossby waves and small-scale orographic gravity waves by subtracting FLAT from TOPO and by subtracting TOPO from TOPO+GW, respectively. We do not perform an integration with only OGWD (but without grid-scale orography) because that seems unphysical; our integrations can be viewed as representing the incremental effects of raising orography while suppressing its influence on the subgrid-scale gravity wave field, then turning on the gravity wave drag. We present averages for boreal winter (December to February) when the orographically induced waves are strongest.

3. Theory

Here we construct a theoretical framework to understand the large-scale precipitation field associated with orographically induced Rossby and gravity waves. We choose to explore the precipitation response indirectly by focusing on the forced vertical motion, which is highly correlated with, and physically coupled to, precipitation. The vertical motion, in turn, is tied to the mean horizontal flow and can be diagnosed using the ω equation, as we will now show. Davies (2015) provides a thorough review of the ω equation together with examples of how it can be used to understand the vertical motion patterns associated with various horizontal flow configurations.

3.1. The moist ω equation

Consider the quasi-geostrophic (QG), hydrostatic, Boussinesq equations of motion on a β -plane with fixed stratification (e.g. Holton and Hakim, 2014, chapter 6),

$$\bar{D}_t \bar{u} - f_0 v - \beta y \bar{v} = F, \tag{1}$$

$$\bar{D}_t \bar{v} + f_0 u + \beta y \bar{u} = 0, \tag{2}$$

$$\bar{D}_t b + N_*^2 w = 0, \tag{3}$$

$$u_x + v_y + w_z = 0. \tag{4}$$

The first two equations are the zonal and meridional momentum equations where (u, v) are velocities in the zonal and meridional (x, y) directions. An overbar denotes a geostrophic quantity and $\bar{D}_t = \partial_t + \bar{u}\partial_x + \bar{v}\partial_y$ is the material derivative following the geostrophic flow. The Coriolis frequency is linearly expanded about latitude ϕ_0 as $f = f_0 + \beta y$, where $f_0 = 2\Omega \sin \phi_0$, Earth’s rotation frequency $\Omega = 2\pi/86400$, $\beta y = 2\Omega \cos \phi_0 y/r_0$, and r_0 is Earth’s radius. F represents an external mechanical forcing, here assumed to be that produced by OGWD. Equation (3) is the moist thermodynamic equation where b is the buoyancy, w is the ageostrophic vertical velocity, and $N_*^2 = (1 - \epsilon)N^2$ is a reduced stratification that approximately accounts for the effects of precipitating convection. The dry stratification, N^2 , is reduced to account for the fact that adiabatic cooling is offset by latent heat release in ascending regions, consistent with convective quasi-equilibrium theories for tropical dynamics (Emanuel *et al.*, 1994). The bulk precipitation efficiency ϵ expresses the fraction of condensed water that falls to the surface: it is zero if all precipitation re-evaporates, unity if all water that condenses falls out of the atmospheric column, and zero for a dry atmosphere in which no latent heating occurs. Boos and Shaw (2013) showed that this approximation of a reduced stratification provides a good description of the precipitation response to OGWD in an idealized GCM. For simplicity, we assume that N^2 and ϵ are fixed. Finally, Eq. (4) is the mass continuity equation, where z denotes the vertical coordinate and subscripts denote partial derivatives.

To obtain a moist ω equation, we add $-f_0\partial_z$ of Eq. (2) to ∂_x of Eq. (3), then add $f_0\partial_z$ of Eq. (1) to ∂_y of Eq. (3). This eliminates

the \bar{D}_t terms in Eqs (1)–(3) through use of thermal wind balance, $f_0\bar{v}_z = b_x$ and $f_0\bar{u}_z = -b_y$. Additional manipulation using the geostrophic continuity relation $\bar{u}_x + \bar{v}_y = 0$ and definition of the vector $\mathbf{Q} = (Q_1, Q_2) = (\bar{u}_x b_x + \bar{v}_x b_y, \bar{u}_y b_x + \bar{v}_y b_y)$ yields a set of two equations,

$$N_*^2 w_x - f_0^2 u_z = f_0 \beta y \bar{u}_z - 2Q_1, \tag{5}$$

$$N_*^2 w_y - f_0^2 v_z = f_0 \beta y \bar{v}_z - 2Q_2 + f_0 F_z. \tag{6}$$

By combining ∂_x of Eq. (5) with ∂_y of Eq. (6) and using Eq. (4), we obtain a moist ω equation,

$$N_*^2 \nabla^2 w + f_0^2 w_{zz} = -2\nabla \cdot \mathbf{Q} + f_0 \beta \bar{v}_z + f_0 F_{yz}, \tag{7}$$

where $\nabla^2 = \partial_{xx} + \partial_{yy}$ is the horizontal Laplacian and $\nabla \cdot = \partial_x + \partial_y$ is the horizontal divergence.

We impose boundary conditions of zero vertical velocity at the top and bottom of the domain. We further assume that the vertical structure of w at least loosely resembles that of a first-baroclinic mode having substantial curvature, w_{zz} , only near the level of maximum w ; at vertical levels distant from this maximum (e.g. in the lower troposphere), Eq. (7) then simplifies to

$$N_*^2 \nabla^2 w \simeq -2\nabla \cdot \mathbf{Q} + f_0 \beta \bar{v}_z + f_0 F_{yz}. \tag{8}$$

This moist ω equation is essentially the same as the classic dry ω equation but with the dry stratification replaced by a reduced, moist stratification, and the acceleration due to OGWD included.

We will use this moist ω equation to understand the distribution of vertical velocity anomalies induced by Asian orography in a model that uses the fully nonlinear primitive equations on a sphere. The vertical velocity anomalies immediately south of the plateau will be shown to lie poleward of 20° latitude and to be associated with rotational motions having a horizontal scale of at least several thousand kilometres, so the QG approximation that underlies Eq. (7) is expected to hold. In a later section of this article, we will additionally comment on shifts in tropical precipitation produced by the orographic forcing; those changes lie outside the domain of validity of the QG ω equation, and will be interpreted using results from previous studies (Shaw and Boos, 2012; Boos and Shaw, 2013) that used theoretical models formulated on an equatorial β -plane.

3.2. Ascent in stationary Rossby waves

On a β -plane, flow over orography induces Rossby waves due to the conservation of potential vorticity (e.g. Holton and Hakim, 2014, Chapter 4). With no momentum forcing ($F = 0$), the vertical velocity can then be diagnosed solely from the divergence of \mathbf{Q} and the β -term that is non-zero in the presence of longitudinal temperature gradients (since $\bar{v}_z \propto b_x$).

To simplify analysis, we assume that meridional variations in temperature are much larger than zonal variations, i.e. $b \simeq b(y)$, with b_y negative and constant and our region of interest lying in the Northern Hemisphere. Then $\mathbf{Q} \simeq (\bar{v}_x b_y, \bar{v}_y b_y) = -|b_y|(\bar{v}_x, \bar{v}_y)$, and the right-hand side of Eq. (8) is well approximated by $2|b_y|\nabla^2 \bar{v}$. We further assume that eastward flow over the large-scale orography induces a zonally elongated wave train of positive and negative vorticity gyres, so that along a latitude circle through the centre of this wave train the zonal derivatives of \bar{v} dominate \mathbf{Q} . In this idealized, zonally elongated wave train, the moist ω equation, Eq. (8), simplifies to

$$N_*^2 \nabla^2 w = 2|b_y|\bar{v}_{xx}. \tag{9}$$

For example, across a cyclone $\bar{v}_x > 0$, while across an anticyclone $\bar{v}_x < 0$. Thus, east of a cyclone $\bar{v}_{xx} < 0$ and ascent is expected, while to the west $\bar{v}_{xx} > 0$ and descent is expected. The locations of these vertical motions in the orographic Rossby wave train are illustrated in Figure 2.

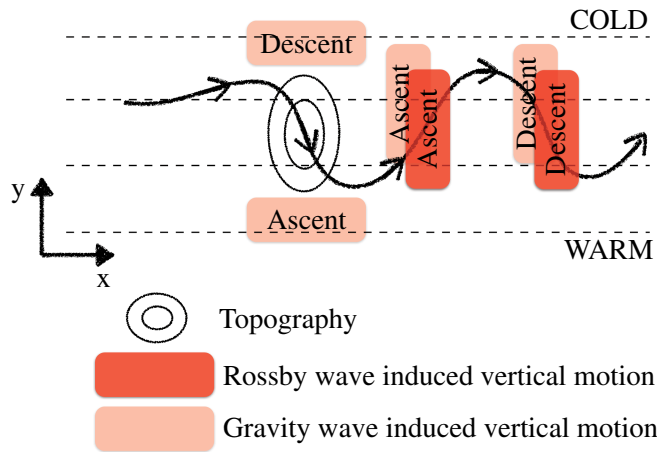


Figure 2. An illustration of the large-scale vertical motions induced by orographically forced Rossby waves and orographic gravity wave drag. Additional ascent on the upstream side of the orography and descent on the downstream side are not shown. [Colour figure can be viewed at wileyonlinelibrary.com].

To estimate the amplitude of vertical motion in the Rossby wave, we assume a plane wave solution by writing $(\tilde{v}, w) = (\tilde{v}, \tilde{w}) \exp(ikx)$, where k is a zonal wave number, and for simplicity we assume that the amplitudes (\tilde{v}, \tilde{w}) are constants.* Then

$$-N_*^2 k^2 \tilde{w} = -2|b_y| k^2 \tilde{v}, \quad (10)$$

and hence

$$w = \frac{2|b_y| \tilde{v}}{N_*^2} \exp(ikx). \quad (11)$$

This confirms that ascent is expected in regions of poleward motion. Furthermore, w is amplified as ϵ becomes larger; diabatic warming reduces the effective stratification as a larger fraction of the water condensing in updraughts precipitates without re-evaporation. We estimate a rough scale for the basic state buoyancy gradient of $b_y \sim 1.5 \times 10^{-7} \text{ m s}^{-2}$ by using thermal wind balance at 30°N with a 20 m s^{-1} change in zonal wind speed over 10 km of altitude. We also use scales of $\tilde{v} \sim 1 \text{ m s}^{-1}$, $N_*^2 \sim 10^{-4} \text{ s}^{-2}$, and $\epsilon = 0$ for a dry atmosphere and $\epsilon = 0.9$ for a moist atmosphere. This yields

$$|w|_{\text{dry}}^{\text{RW}} \sim 0.3 \text{ cm s}^{-1}, \quad |w|_{\text{moist}}^{\text{RW}} \sim 3 \text{ cm s}^{-1}. \quad (12)$$

3.3. Ascent forced by orographic gravity wave drag

In a stratified atmosphere, flow over orography also induces gravity waves (e.g. Sutherland, 2010). These waves can propagate vertically to high altitudes and their associated momentum flux can significantly alter the momentum budget of the atmosphere (e.g. Andrews *et al.*, 1987). In the above equations, we used F to represent the acceleration of the large-scale flow by the net effects of gravity wave breaking at smaller scales (these smaller scales would be unresolved in a typical GCM).

We first consider the case in which horizontal temperature gradients are weak near the orography (i.e. $b_x \simeq b_y \simeq 0$). It follows that Eq. (8) reduces to

$$N_*^2 \nabla^2 w \simeq f_0 F_{yz}. \quad (13)$$

A subtropical, upper-tropospheric westward force is known to produce ascent on the equatorial side of the forcing and

subsidence on the poleward side in what is known as the ‘downward control’ response (Haynes *et al.*, 1991). Shaw and Boos (2012) showed that the ascent and subsidence become strongly localized in longitude when the momentum forcing is localized in longitude, in both dry and moist models (Boos and Shaw, 2013). Thus, although the phrase ‘downward control’ is traditionally used to describe the zonal-mean response to a zonal-mean upper-level torque, here we also use it to refer to the zonally confined ascent that occurs in response to a zonally confined torque. For such a horizontally confined wave drag with a vertical structure similar to that of a first-baroclinic mode (as in Boos and Shaw, 2013), we can use Eq. (13) to show that the vertical velocity induced by F scales as

$$w \sim -\frac{f_0 A L}{4\pi^2 H N_*^2},$$

where A is the retrograde wave drag amplitude, L the horizontal scale of the drag, and H the vertical scale. A rough estimate of the vertical velocity amplitude can be achieved by using these approximate scales for a wave drag at 30°N : $A \sim -30 \text{ m s}^{-1} \text{ day}^{-1}$, $L \sim 10^\circ$ longitude, $H \sim 10 \text{ km}$, and $N_*^2 \sim 10^{-4} \text{ s}^{-2}$. The amplitude of $-30 \text{ m s}^{-1} \text{ day}^{-1}$ is meant to represent the peak upper-level strength of the drag localized over Asian orography, and is consistent with typical estimates of the zonal mean OGWD being about an order of magnitude smaller (e.g. Palmer *et al.*, 1986; McFarlane, 1987; Shaw and Boos, 2012); this amplitude is also consistent with the peak parametrized OGWD at 100 hPa over Tibet in CESM (see next section). Again using $\epsilon = 0$ for a dry atmosphere and $\epsilon = 0.9$ for a moist atmosphere yields the vertical velocity scales

$$|w|_{\text{dry}}^{\text{GW}} \sim 0.1 \text{ cm s}^{-1}, \quad |w|_{\text{moist}}^{\text{GW}} \sim 1 \text{ cm s}^{-1}. \quad (14)$$

In the presence of a basic state temperature gradient ($b_y \neq 0$), one also needs to account for the effect of the wave drag on the divergence of \mathbf{Q} . By taking the curl of the horizontal momentum Eqs (1) and (2), it becomes clear that a localized, single-signed torque will force a meridional dipole in relative vorticity, i.e. $\bar{D}_t(\tilde{v}_x - \tilde{u}_y) + \dots = -F_y$. This vortex dipole will be advected by the mean zonal flow (which is non-zero because $b_y \neq 0$); more importantly, in the presence of a horizontal temperature gradient, it will also be accompanied by vertical motions described by the ω equation. Similar to the case of stationary Rossby waves, one would expect to see ascent downshear of cyclonic parts of the flow. The exact location of these regions of ascent and subsidence will depend on the wavelength of the stationary Rossby wave excited by the torque and on how the mean flow refracts that Rossby wave. OGWD can thus be viewed as directly forcing vertical motions through a localized downward control mechanism, and indirectly producing vertical motions through the QG ascent and subsidence that occur in Rossby waves excited by the wave drag.

Figure 2 illustrates the locations of the expected vertical motions due to the OGWD. The meridional dipole of ascent and subsidence that is centred on the orographic forcing is the localized downward control response that has been well examined in previous studies. The alternating regions of ascent and subsidence downstream (east) of the orography are more speculative, and their magnitude and location will depend greatly on the interaction of the forced vorticity dipole with the basic state flow. These might interfere, constructively or destructively, with the vertical motions that accompany the stationary Rossby wave discussed in the previous subsection. Their phasing with the ascent anomalies discussed in section 3.2 likely depends on the length-scales and positions of the OGWD and the forcing for the stationary Rossby wave.

In the next section, we use the theoretical ideas developed here to understand better the flow perturbations caused by the Tibetan Plateau during boreal winter, as represented by a comprehensive model that includes parametrizations of both OGWD and moist processes.

*In this article, we emphasize the role of stationary waves. The contribution of transient baroclinic disturbances may be significant if orography or the induced stationary wave alter the characteristics of those disturbances, but that goes beyond the scope of this article.

4. Results

Without the Asian orographic forcing, the climatological mean surface wind would largely flow from southwest to northeast during boreal winter over central and northern Asia, as evidenced by results from our FLAT integration (Figure 3). The extratropical temperature field has a prominent meridional gradient in this model ($T_y < 0$, $T_x \sim 0$), consistent with assumptions about the basic state made in the previous section on the ascent in orographically forced Rossby waves.

We isolated the effect of large-scale orographic Rossby waves by subtracting the FLAT integration from the TOPO integration and examining differences that are significant at the 5% level. Flow over Asian orography generates a stationary Rossby wave train with a cyclonic gyre immediately to the east of the orography and an anticyclonic gyre to the northwest, as evidenced by the anomalous 300 hPa geopotential height, which is the streamfunction for the geostrophic wind at that level (Figure 4(a)). As expected from the diagnostic ω equation, there is ascent to the east of the cyclone and descent to the west. Unsurprisingly, the precipitation anomaly is positively correlated with the vertical velocity anomaly, with stronger precipitation anomalies at lower latitudes where moisture is more abundant (Figure 4(c)). The Rossby wave train bends southward to the east of the orography and penetrates deep into the Tropics, which can be understood in terms of the refraction of linear, stationary Rossby waves by the zonal mean basic state (Nigam *et al.*, 1988; Cook and Held, 1992). This wave train has a structure that is highly similar to that of dry, nonlinear solutions for the response to an idealized, isolated, midlatitude mountain and to realistic Asian orography (Held *et al.*, 2002), indicating the utility of linear theory. In addition to the aforementioned high and low geopotential anomalies immediately adjacent to the orography, this wave train also contains a high over the northwest Pacific (centred near 30°N, 160°E), with an anomalous ascent to the west and subsidence to the east of that oceanic high. The orographic Rossby wave train thus brings more rainfall to the ocean around Japan and less to northern and central Asia.

There is also a strong positive anomaly of ascent and precipitation a few degrees north of the Equator (between 90°E and 180°E). The dynamics responsible for this anomaly may seem less obvious but are consistent with ascent occurring on the upshear side of an anticyclone. The direction of the vertical shear changes from eastward to northward as one moves from 30°N to the Equator in the West Pacific (e.g. the temperature gradient near 120°E in Figure 3), so the QG ω equation would predict ascent and

subsidence, respectively, to the west and east of the anomalous West Pacific high at 30°N, while it would predict ascent on the southern edge of that high close to the Equator. Of course, the QG ω equation is not expected to be quantitatively accurate at very low latitudes, but it might correctly predict the sign of the vertical motion anomaly at, say, 10°N. Due to the warmest waters and thus the highest humidities lying near the Equator, the largest precipitation anomaly lies remote from the orographic forcing over the southern edge of that anomalous West Pacific high (Figure 4(c)). Strong equatorial anomalies in rainfall were seen in the moist response to an idealized midlatitude mountain simulated by Wills and Schneider (2016), although these were located at somewhat different zonal locations relative to the imposed orography than in our simulations; this difference might arise from differences in the basic state or in the amplitude of the orographic forcing (our peak surface heights are about twice theirs and our near-equatorial precipitation anomalies are roughly a factor of 4 larger). The main point is that extratropical orographic forcings can produce a strong, non-local rainfall response that stretches deep into the Tropics and that can be understood, at least qualitatively, using the QG ω equation applied to a forced, stationary Rossby wave.

Gravity waves are also excited as winds flow over highly variable Asian orography. These waves are generated at the surface, but they flux zonal momentum across stratification surfaces to high altitudes where they break and decelerate the larger-scale flow (e.g. Fritts and Alexander, 2003). The gravity wave parametrization used in CESM (McFarlane, 1987) assumes that momentum deposition is required to inhibit convective instability. This process is parametrized by requiring a low non-dimensional Froude number which, in turn, is inversely proportional to the resolved zonal wind and air density. Thus, momentum deposition is expected at high altitudes above the maximum jet location, where zonal wind and density both decrease with height. Indeed, Figure 4(b) shows large deceleration (i.e. deposition of westward momentum) over Tibet at 100 hPa.

In section 3, this acceleration was denoted by F and was argued to produce ascent to the south and descent to the north of the upper-level westward forcing. That idealized, theoretical result is consistent with the anomalous vertical motion produced by the OGWD parametrization (Figure 4(b) shows the statistically significant difference between TOPO+GW and TOPO). The anomalous vertical motion is accompanied by anomalous precipitation, with larger rainfall anomalies occurring closer to the Equator (Figure 4(d)). The peak anomalies produced by the OGWD have magnitudes roughly one-third of those generated by the orographic Rossby wave but can dominate in select regions. The OGWD enhances precipitation over much of south Asia and in a zonally elongated band in the northern Bay of Bengal and West Pacific. Anomalous descent and suppressed precipitation occur northwest, rather than directly north, of the forcing; Boos and Shaw (2013) also found that anomalous descent did not take place directly poleward of the forcing in idealized models, but could be offset in either zonal direction depending on model details and the basic state. There is also a zonally elongated band of anomalous subsidence and suppressed rainfall over the Equator, which together with the band of anomalous precipitating ascent near 10°N indicates a northward shift of the ITCZ. While enhanced ascent in the basic state ITCZ is expected since the ITCZ lies on the equatorial side of the torque and the ascent response will be amplified in humid, precipitating regions due to the reduced moist static stability there, the anomalous subsidence that accompanies the ITCZ shift is less straightforward to explain. Nevertheless, Boos and Shaw (2013) found a clear poleward shift in the equatorial ITCZ in response to a subtropical westward momentum forcing, and attributed this change to a reduction in equatorial eddy momentum flux convergence induced by the forcing.

The wave drag also induces a series of cyclones and anticyclones – a Rossby wave train – which alters vertical

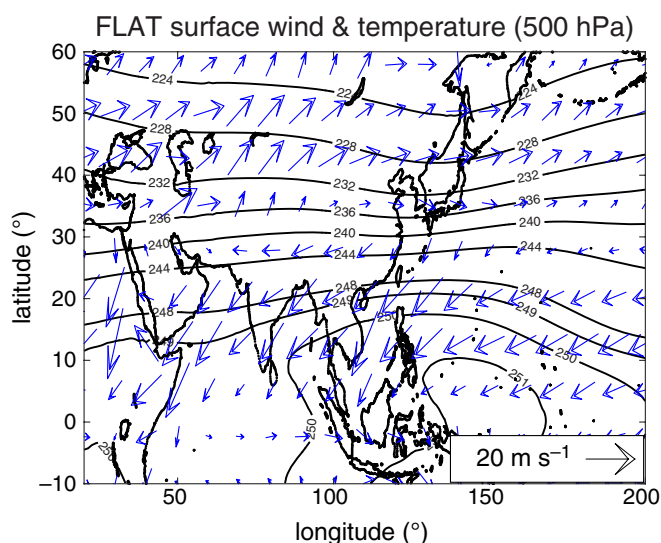


Figure 3. The simulated climatological surface wind (m s^{-1} , arrows) and 500 hPa temperature field (K, contours) during boreal winter for the FLAT integration (with the large-scale orography removed and the gravity wave drag parametrization turned off). [Colour figure can be viewed at wileyonlinelibrary.com].

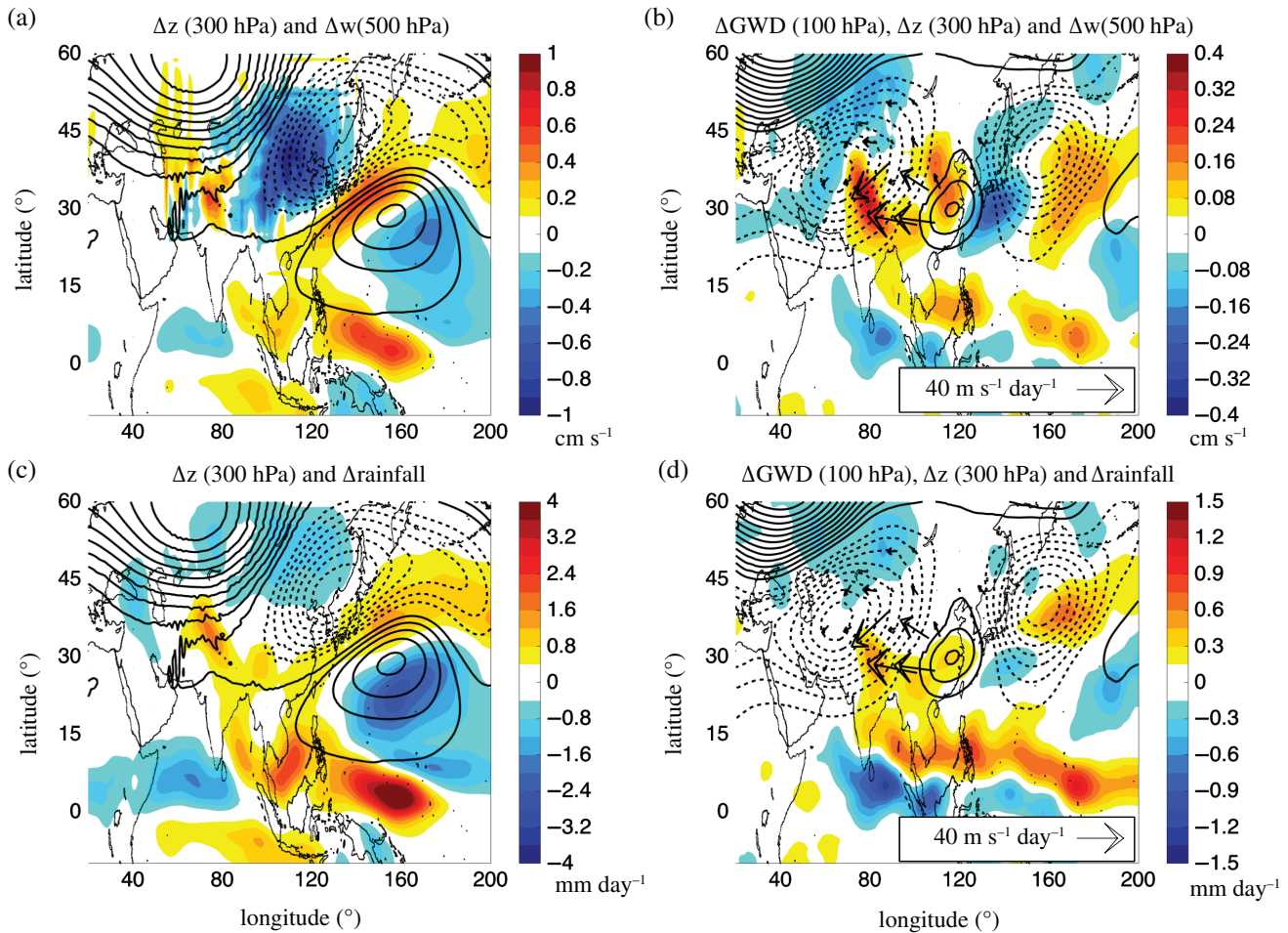


Figure 4. The large-scale effects of orographically forced Rossby waves and orographic gravity wave drag on geopotential height, vertical motion, and precipitation. (a) and (c) show the isolated effect of the stationary Rossby wave directly forced by orography, obtained by subtracting the FLAT from TOPO integration. (b) and (d) show the isolated effect of orographic gravity wave drag obtained by subtracting the TOPO from TOPO+GW integration. (a) and (b) show the change in geopotential height at 300 hPa (black contours, m) and 500 hPa vertical velocity (shading, cm s^{-1}). (c) and (d) show the change in 300 hPa geopotential height (black contours) and precipitation (shading, mm day^{-1}). The gravity wave drag is denoted by arrows in (b) and (d). Solid (dashed) contours show positive (negative) values. The contour interval in (a) and (c) is 20 m while in (b) and (d) it is 5 m. All panels show only statistically significant differences (at the 5% confidence level) computed using a bootstrap method with 200 iterations.

motion and rainfall in the presence of the wintertime meridional temperature gradient. Immediately east of the momentum forcing there is a small anticyclone (centred at 120°E , 30°N) with subsidence to its east, and east of that there is a cyclone with ascent to its east (Figure 4(b)). The phasing of the vertical motion and horizontal wind anomalies is as described in our preceding theory section. As mentioned there, the exact location of these downstream vertical motion anomalies is expected to depend on the time-mean wind as well as the length-scales and positions of the OGWD and the large-scale orography. For example, the OGWD peaks in the region of large surface height variance around the edges of the Tibetan Plateau (Figure 1 of Cohen and Boos, 2016), while the Mongolian Plateau north of Tibet has been argued to be most important for influencing the Asian winter jet stream (Shi *et al.*, 2015; White *et al.*, 2016).

The location of the geopotential anomalies west of the OGWD forcing deserves some explanation. At 100 hPa, where the OGWD is strongest, there is strong westward flow in the region of the forcing (not shown). When one descends to 300 hPa, the response is dominated by poleward flow in the area of the forcing; this poleward flow is part of the localized downward control response and is also part of a cyclone that lies immediately west of the forcing (Figure 4(b)). In other words, the reaction to the momentum forcing projects onto both divergent and rotational winds. Further to the northwest is the strongest geopotential anomaly, which is zonally elongated and is in geostrophic balance with a westward wind anomaly that stretches over all of Asia near 50°N . This is part of a zonal mean shift in the extratropical jet that occurs in response to the momentum forcing; meridional shifts

in the zonal mean extratropical jet were prevalent in the idealized models of Shaw and Boos (2012) and Boos and Shaw (2013).

5. Summary and discussion

Although much of continental Asia is dry in boreal winter, some parts of Asia and large areas of the Indo-West Pacific Ocean receive the majority of their annual precipitation during that season. Earlier studies have shown that orography influences Asian precipitation during boreal winter, producing strong zonal asymmetries (e.g. Manabe and Terpstra, 1974; Broccoli and Manabe, 1992; Wills and Schneider, 2015, 2016). However, the dynamics responsible for the precipitation response to Rossby and gravity waves forced by realistic orography have not been previously examined in a unified framework and have remained incompletely understood.

Starting with what is essentially a summary and extension of previous theories, we showed that both orographically forced stationary Rossby and gravity waves are expected to exert significant and distinct influences on the large-scale structures of vertical motion and precipitation. Then we used these theoretical concepts to understand the detailed response to Asian orography during boreal winter, as simulated by a comprehensive numerical model.

Similar to Manabe and Terpstra (1974, their Figure 9.1), we find that the stationary Rossby wave which is directly forced by Asian orography enhances precipitation over the West Pacific near Japan but reduces precipitation over much of northern and central Asia. Unlike previous studies of the stationary Rossby

wave response to orography, we show clearly that the vertical velocity and rainfall patterns follow nicely from the diagnostic ω equation applied to the Rossby wave train. The precipitation perturbations are non-local and appear to be weighted by the basic state moisture content, with precipitation increasing over parts of south Asia and just north of the Equator in the West Pacific and East Indian Oceans (Figure 4(c)). Our arguments implicitly assume that time-mean vertical velocity anomalies determine the precipitation response to first order, with the contribution of transients being comparatively small. The general correspondence between vertical motion and precipitation anomalies in our integrations qualitatively supports this, though there are certain regions where precipitation changes do not exactly follow time-mean vertical velocity changes (e.g. over central Asia near 60°N in Figures 4(a) and (c)). Broccoli and Manabe (1992) suggested that precipitation might be suppressed upstream of troughs in orographically induced stationary waves because of both time-mean subsidence and the suppression of storm development, but Wills and Schneider (2016) found that most anomalies in vertically integrated moisture flux convergence created by a midlatitude mountain in an idealized GCM were associated with the time-mean ascent.

Orographically induced gravity wave drag influences the precipitation field significantly during boreal winter, as the wave drag over Tibet is significant during that season (Figures 4(b), (d) and Cohen and Boos, 2016). The peak precipitation anomalies caused by the wave drag have amplitudes that are only one-third as large as those produced by the direct Rossby wave response to the orography, but the response to the wave drag can dominate in particular regions. The precipitation response to the OGWD is distinct and can be understood in terms of a zonally confined downward control response to the westward forcing, combined with the QG vertical motions that occur in the Rossby wave train excited by the gravity wave drag. The localized downward control mechanism suppresses precipitation over northwest Asia, enhances it over most of south Asia, and produces a poleward shift of the ITCZ over the near-equatorial Indo-West Pacific Ocean (Figure 4(d)). Many of these features of the precipitation response were predicted by Boos and Shaw (2013), but it was not obvious that results from their idealized models, which had zonally symmetric boundary conditions and an entirely oceanic lower boundary, would be relevant in more realistic models; furthermore, the forcing used by Shaw and Boos (2012) and Boos and Shaw (2013) was an imposed westward acceleration rather than a drag on the upper-level flow.

While the direct Rossby wave response to the continental-scale orographic forcing may be well-resolved and thus well-simulated by GCMs, the gravity wave drag is entirely parametrized in our model and may contain significant errors. Indeed, Cohen and Boos (2016) found substantial differences in the magnitude and vertical structure of the climatological mean gravity wave drag over Asia parametrized by two different atmospheric reanalyses; the error in GCMs may be even larger because their grid-scale winds are not constrained by observations. Thus, the magnitude of the OGWD forcing in our GCM and the associated precipitation response may be greatly overestimated or underestimated. Although it is in some ways artificial to partition the precipitation response to orography into that produced by a directly forced Rossby wave and that generated by gravity wave drag, this partitioning may be useful until parametrizations of OGWD are better constrained.

Acknowledgements

Both authors acknowledge support from National Science Foundation award AGS-1515960 and Office of Naval Research award N00014-15-1-2531. NYC also acknowledges partial support from National Science Foundation award AGS-1317469.

References

- Alexander MJ, Geller M, McLandress C, Polavarapu S, Preusse P, Sassi F, Sato K, Eckermann S, Ern M, Hertzog A, Kawatani Y, Pulido M, Shaw TA, Sigmund M, Vincent R, Watanabe S. 2010. Recent developments in gravity-wave effects in climate models and the global distribution of gravity-wave momentum flux from observations and models. *Q. J. R. Meteorol. Soc.* **136**: 1103–1124.
- Andrews DG, Holton JR, Leovy CB. 1987. *Middle Atmosphere Dynamics*, Vol. 40. Academic Press: Cambridge, MA.
- Boos WR. 2015. A review of recent progress on Tibet's role in the South Asian monsoon. *CLIVAR Exch. No. 66* **19**: 23–27.
- Boos WR, Shaw TA. 2013. The effect of moist convection on the tropospheric response to tropical and subtropical zonally asymmetric torques. *J. Atmos. Sci.* **70**: 4089–4111.
- Broccoli A, Manabe S. 1992. The effects of orography on midlatitude northern hemisphere dry climates. *J. Clim.* **5**: 1181–1201.
- Bühler O. 2014. *Waves and Mean Flows*. Cambridge University Press: Cambridge, UK.
- Cohen NY, Boos WR. 2016. Modulation of subtropical stratospheric gravity waves by equatorial rainfall. *Geophys. Res. Lett.* **43**: 466–471, doi: 10.1002/2015GL067028.
- Cohen NY, Gerber EP, Bühler O. 2014. What drives the Brewer–Dobson circulation? *J. Atmos. Sci.* **71**: 3837–3855.
- Cook KH, Held IM. 1992. The stationary response to large-scale orography in a general circulation model and a linear model. *J. Atmos. Sci.* **49**: 525–539.
- Davies HC. 2015. The Quasigeostrophic Omega equation: Reappraisal, refinements, and relevance. *Mon. Weather Rev.* **143**: 3–25.
- Emanuel KA, Neelin DJ, Bretherton CS. 1994. On large-scale circulations in convecting atmospheres. *Q. J. R. Meteorol. Soc.* **120**: 1111–1143.
- Fritts DC, Alexander MJ. 2003. Gravity wave dynamics and effects in the middle atmosphere. *Rev. Geophys.* **41**: 1003, doi: 10.1029/2001RG000106.
- Haynes P, McIntyre M, Shepherd T, Marks C, Shine KP. 1991. On the 'downward control' of extratropical diabatic circulations by eddy-induced mean zonal forces. *J. Atmos. Sci.* **48**: 651–678.
- Held IM, Ting M, Wang H. 2002. Northern winter stationary waves: Theory and modeling. *J. Clim.* **15**: 2125–2144.
- Holton JR, Hakim GJ. 2014. *An Introduction to Dynamic Meteorology*, Vol. 88. Academic Press: Cambridge, MA.
- Ma D, Boos WR, Kuang Z. 2014. Effects of orography and surface heat fluxes on the South Asian summer monsoon. *J. Clim.* **27**: 6647–6659.
- McFarlane N. 1987. The effect of orographically excited gravity wave drag on the general circulation of the lower stratosphere and troposphere. *J. Atmos. Sci.* **44**: 1775–1800.
- Manabe S, Terpstra TB. 1974. The effects of mountains on the general circulation of the atmosphere as identified by numerical experiments. *J. Atmos. Sci.* **31**: 3–42.
- Nigam S, Held IM, Lyons SW. 1988. Linear simulation of the stationary eddies in a GCM. Part II: The 'mountain' model. *J. Atmos. Sci.* **45**: 1433–1452.
- Palmer TN, Shutts GJ, Swinbank R. 1986. Alleviation of a systematic westerly bias in general circulation and numerical weather prediction models through an orographic gravity wave drag parametrization. *Q. J. R. Meteorol. Soc.* **112**: 1001–1039.
- Rodwell MJ, Hoskins BJ. 2001. Subtropical anticyclones and summer monsoons. *J. Clim.* **14**: 3192–3211.
- Shaw TA, Boos WR. 2012. The tropospheric response to tropical and subtropical zonally asymmetric torques: Analytical and idealized numerical model results. *J. Atmos. Sci.* **69**: 214–235.
- Shi Z, Liu X, Liu Y, Sha Y, Xu T. 2015. Impact of Mongolian Plateau versus Tibetan Plateau on the westerly jet over North Pacific Ocean. *Clim. Dyn.* **44**: 3067–3076.
- Stephenson DB. 1994. The northern hemisphere tropospheric response to changes in the gravity-wave drag scheme in a perpetual January GCM. *Q. J. R. Meteorol. Soc.* **120**: 699–712.
- Sutherland BR. 2010. *Internal Gravity Waves*. Cambridge University Press: Cambridge, UK.
- Teixeira MAC. 2014. The physics of orographic gravity wave drag. *Front. Phys.* **2**: 1–24, doi: 10.3389/fphy.2014.00043.
- Trenberth KE, Chen SC. 1988. Planetary waves kinematically forced by Himalayan orography. *J. Atmos. Sci.* **45**: 2934–2948.
- White RH, Battisti DS, Roe GH. 2016. Mongolian mountains matter most: Implications of the latitude and shape of Asian orography on the winter Pacific jet stream. *J. Clim.* In Press.
- Wills RC, Schneider T. 2015. Stationary eddies and the zonal asymmetry of net precipitation and ocean freshwater forcing. *J. Clim.* **28**: 5115–5133.
- Wills RC, Schneider T. 2016. How stationary eddies shape changes in the hydrological cycle: Zonally asymmetric experiments in an idealized GCM. *J. Clim.* **29**: 3161–3179.
- Wu G, Liu Y, He B, Bao Q, Duan A, Jin FF. 2012. Thermal controls on the Asian summer monsoon. *Sci. Rep.* **2**: 404.
- Yanai M, Wu GX. 2006. *The Asian Monsoon*. Springer: Berlin.